Gexia-Zhuyu Decoction Attenuates Carbon Tetrachloride-Induced Liver Fibrosis in Mice Partly via Liver Angiogenesis Mediated by Myeloid Cells

Authors' Contribution:
Study Design A
Data Collection B
Statistical Analysis C
Data Interpretation D
Manuscript Preparation E
Literature Search F
Funds Collection G

ABDF Zhengming Deng*
ACF   Shihu Zhang*
BDE   Shaohua Ge
BF   Fanping Kong
ACEG Shibing Cao
CE   Zhaoxia Pan

Department of General Surgery, Affiliated Hospital of Nanjing University of Chinese Medicine, Nanjing, Jiangsu, P.R. China

Corresponding Authors:
Source of support:

* Zhengming Deng and Shihu Zhang contributed equally to this work
Shibing Cao, e-mail: doc99cao@sina.com, Zhaoxia Pan, e-mail: pan7076@163.com
This study was funded by the National Natural Science Foundation of China (No. 8147097)

Background: This study aims to demonstrate the underlying correlation between the resolution of liver fibrosis induced by Gexia-Zhuyu decoction (GZD) treatment and myeloid cell-mediated angiogenesis.

Material/Methods: A liver fibrosis mouse model induced by carbon tetrachloride (CCl_4) intervention was employed in this study. Dynamics of blood liver function parameters were followed. The liver pathology was detected by Sirius Red and Masson staining. Matrix metalloproteinase (MMP) 2/9, tissue inhibitors of metalloproteinase (TIMP)-1/2, and vascular endothelial growth factor (VEGF)-A expression levels were measured. Bone marrow chimera mice were generated by transfer of bone morrow cells from green fluorescent protein (GFP)-knockin mice into irradiated wild-type mice, and were used it to visualize the role of myeloid cells on the fibrosis resolution induced by GZD treatment.

Results: The result of Sirius Red and Masson staining and the dynamics of blood liver function parameters showed that 5 weeks of GZD treatment attenuated the severity of liver fibrosis with continual CCl_4 administration. GZD treatment promoted the expression of MMP2/9 and repressed the heightened level of TIMP-1/2 in the recovery phase. More notably, the increased VEGF-A and augmented endothelial progenitor cells were observed in the liver and blood in mice that received GZD, and contributed to the remodeling of hepatic vascular though the CXCL12/CXCR4 axis. Then, chimera mice with GFP-positive bone marrow cells were used to show angiogenesis driven by GZD-induced myeloid cell motivation. We found that GZD facilitated myeloid cells binding to the vascular CXCR4 and induced the resolution of fibrosis.

Conclusions: This study shows that activation of myeloid cells induced by GZD administration accelerates the functional angiogenesis, which benefits the resolution of CCl_4-induced liver fibrosis.

MeSH Keywords: Fibrosis • Liver • Myeloid Cells

Abbreviations: **GZD** – Gexia-Zhuyu decoction; **CCl4** – carbon tetrachloride; **MMP** – matrix metalloproteinase; **TIMP** – tissue inhibitors of metalloproteinase; **VEGF** – vascular endothelial growth factor; **GFP** – green fluorescent protein; **HBV** – hepatitis B virus; **ECM** – extracellular matrix; **EPCs** – endothelial progenitor cells; **PBS** – phosphate-buffered saline; **HPLC** – high-performance liquid chromatography; **ELISA** – enzyme-linked immunosorbent assay; **PDGF** – platelet-derived growth factor; **TGF-**β – transforming growth factor-β1

Full-text PDF: https://www.medscimonit.com/abstract/index/idArt/913481

📄 3085   ▦ 2   📊 5   📖 24

Background

Liver fibrosis, which is the outcome of the disequilibrium between extracellular matrix hyperplasia and degradation, is a common characteristic of chronic liver diseases caused by multiple factors, including chronic hepatitis B virus (HBV) or hepatitis C virus infection, autoimmune hepatitis, and steato-hepatitis [1,2]. Previous studies confirm that liver fibrogenesis is highly related to the excess activation of hepatic stellate cells and deposition of extracellular matrix (ECM) [3]. Further evidence indicates that chronic liver diseases are consistent with the remodeling of intra-hepatic vasculature, suggesting that inhibition of excessively pathological angiogenesis may limit liver fibrogenesis in the progressive stage [4]. Indeed, sinusoids, unique microvasculature that consists of liver sinusoidal endothelial cells and hepatocytes, are abundant in the liver. The liver sinusoidal endothelial cells are account for about 1/5 of all liver cells. However, new pathological vessels in the region of fibrosis are immature and redundant, and cause an extra burden on liver circulation [5,6]. Therefore, anti-angiogenic therapy is considered to treat fibrogenesis during the progressive stage of chronic liver diseases to prevent the pathological alteration. Conversely, Kantari-Mimoun et al. [7] suggested that pro-angiogenesis cytokine vascular endothelial growth factor (VEGF) secreted by myeloid cells contributes to the resolution of liver fibrosis in which the etiological factor was removed. Thus, we hypothesized from another perspective that a traditional Chinese medicine used in the treatment of liver fibrosis with the effect of activating circulation to remove blood stasis might be effective in promoting myeloid-cell-driven functional angiogenesis.

Gexia-Zhuyu decoction (GZD), which is widely used to treat chronic liver diseases such as cirrhosis and liver fibrosis, was employed to treat carbon tetrachloride (CCl4)-induced liver fibrosis in this study. Previous investigation with GZD showed that administration of GZD prevents the process of dimethyl-nitrosamine-induced liver fibrosis in rats by inhibiting the proliferation of hepatic stellate cells [8]. We set out to assess the role of functional angiogenesis by performing a dynamic study of liver function. Then, the activity of functional angiogenesis and the activation of myeloid cells in the recovery phase of fibrosis were tracked. In addition, the number of endothelial progenitor cells (EPCs), a unique myeloid cell subset with the function of promoting re-establishment of the sinusoidal epithelium, were measured by flow cytometry [9]. A bone marrow chimera mouse model was constructed by transferring bone marrow cells from green fluorescent protein (GFP)-knockin mice into irradiated wild-type mice to trace myeloid-derived cells homing to the liver.

In the present study, we identified the underlying mechanism between functional angiogenesis and GZD induced-liver fibrosis resolution in a CCl4-induced liver fibrosis mouse model and showed that GZD treatment accelerated myeloid cell homing to the liver via the CXCL12/CXCR4 axis.

Material and Methods

Animals

We purchased 8-week-old female C57BL/6J mice and eGFP C57BL/6J mice from Nanjing Biomedical Research Institute of Nanjing University. Experimental protocols were approved by the Committee on Laboratory Animal Care of Nanjing University of Chinese Medicine, and all mice were given humane care according to the guidelines of the National Institutes of Health (USA).

Generation of bone marrow chimeric mice

Bone marrow chimeric mice were generated in the Nanjing Biomedical Research Institute of Nanjing University. Bone marrow was collected from the femurs and tibia of eGFP mice, and was suspended in phosphate-buffered saline (PBS). Then, cell suspensions were filtered through a 40-μm filter. After centrifugation, the cells were re-suspended in saline at the concentration of 2×10^7/mL. The wild-type recipient mice were exposed to irradiation and then received 1×10^7 bone marrow cells from donor mice intravenously. The mice were fed at least 4 weeks before the following experiments were performed.

Modified Gexia-Zhuyu decoction preparation

All herbal medicinal plants were obtained from Jiangsu Provincial Hospital of Traditional Chinese Medicine. The modified GZD contains 10 kinds of medicinal materials, including 20 g Red Paeony Root, 10 g Radix Salviae Miltiorrhizae, 10 g Angelica Sinensis, 10 g Leech, 10 g Semen Persicae 15 g Eupolyphaga sinensis, 10 g Crocus sativus Linn, 10 g Pericarpium Arecae, 10 g Fructus Aurantii, and 10 g Vinegar-baked Bupleurum Root. The mixture was extracted with 10 times volume of boiling sterile water. Then, the decoction was filtered through a nylon mesh to remove the residue, and lyophilized. The powder was stored at −80°C for the following oral administration.

High-performance liquid chromatography analysis

The GZD powder was dissolved in water and filtered through a 0.22-mm filter before loading into the high-performance liquid chromatography (HPLC) system. The analysis was performed with a Cosmosil 5C18-AR-II column (250 mm × 4.6 mm). Paeoniflorin and glycyrrhizin standards (Sigma-Andrich, St. Louis, MO, USA) were used as external controls in the
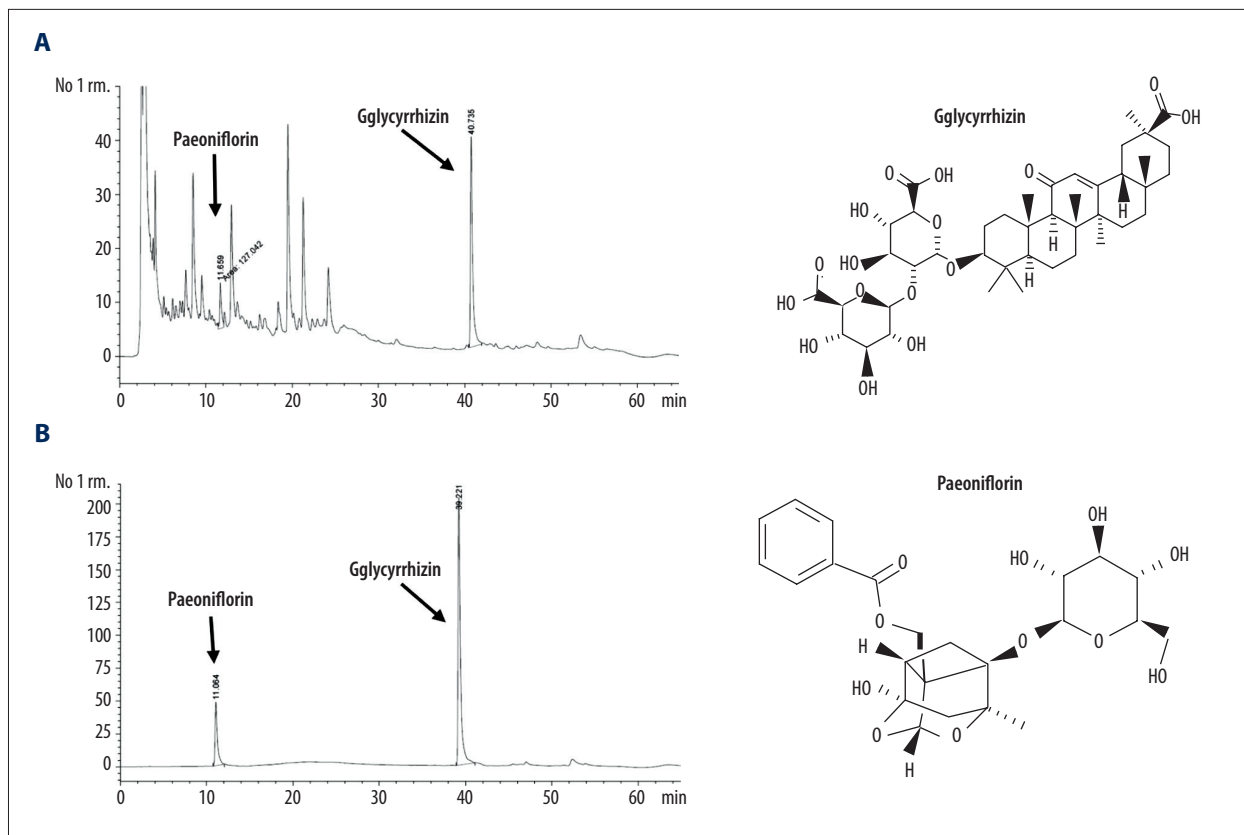
Figure 1. HPLC chromatograms of paeoniflorin and glycyrrhizin in GZD. (**A**) Paeoniflorin and glycyrrhizin were separated from GZD at retention time. (**B**) HPLC chromatogram of paeoniflorin and glycyrrhizin.

HPLC analyses, as shown in Figure 1A, 1B. The mobile phase consisted of acetonitrile-H_3PO4 with a flow rate of 1.0 mL/min.

Animal experiments

The mice in the same batch were divided into 5 groups: control group, nothing administered; GZD+CCl_4 group, received GZD from week 8 to 18 and administrated CCl_4 from week 0 to 18; Mock+CCl_4 group, administrated CCl_4 from week 0 to 18; GZD group, administrated GZD from week 8 to 18 and administrated CCl_4 from week 0 to 8; and Mock group, administrated CCl_4 from week 0 to 8. The mice except for the control group received carbon tetrachloride i.p. 2 times a week for 8 weeks as previously described to induce hepatic fibrosis. Next, mice in the GZD+CCl_4, Mock+CCl_4 groups received continuous treatment with carbon tetrachloride. Oral administration of 400 µL GZD was performed in the GZD+CCl_4 and GZD groups every day for 10 weeks. Experimental schedule and programs detection were performed as shown in Figure 1B. After administration, the animals were sacrificed at week 11 or week 18 by excess ether anesthesia. The livers were weighed and then immediately dissected into appropriate pieces for RNA extraction, protein extraction, and histology.

Histological analysis

Mouse livers were perfused via the portal vein with 8 mL of phosphate-buffered saline (PBS). The excised livers were harvested and fixed in 4% paraformaldehyde. Sirius Red and Masson staining were performed to detect collagen hyperplasia.

Immunofluorescent histology

Frozen sections 8 µm in thickness were cut, fixed with 4% paraformaldehyde for 10 min, and left to dry at ambient temperature. The sections were then incubated with CXCR4 antibody and a Cy3-conjugated goat anti-rabbit Ab (Santa Cruz Biotechnology, Santa Cruz, CA, USA). These slides were washed and incubated with DAPI (4',6-diamidino-2-phenylindole) and mounted with Fluoromount-G (SouthernBiotech, Birmingham, AL, USA). The sections were visualized with a confocal laser scanning microscope (Olympus, Tokyo, Japan).

Real-time quantitative polymerase chain reaction (RT-qPCR)

We homogenized 100 mg of liver tissue in 1 mL TRIzol reagent (Invitrogen, Carlsbad, CA, USA) to extract the total RNA.

Table 1. Q-PCR primers.

Gene		Sequences (5' to 3')
GAPDH	Forward	ACCCAGAAGACTGTGGATGG
GAPDH	Reverse	ACACATTGGGGGTAGGAACA
MMP2	Forward	ACAACAGCTGTACCACCGAG
MMP2	Reverse	AGCTCCTGGATCCCCTTGAT
MMP9	Forward	CAGCCAGACACTAAAGGCCA
MMP9	Reverse	ACAACTCGTCGTCGTCGAAA
MMP13	Forward	ATGTGGAGTGCCTGATGTGG
MMP13	Reverse	ATCAAGGGATAGGGCTGGGT
TIMP1	Forward	CCAGAACCGCAGTGAAGAGT
TIMP1	Reverse	TCTGGTAGTCCTCAGAGCCC
TIMP2	Forward	ATGGCAACCCCATCAAGAGG
TIMP2	Reverse	TCTTTCCTCCAACGTCCAGC
VEGF-A	Forward	GGAGATCCTTCGAGGAGCACTT
VEGF-A	Reverse	GGCGATTTAGCAGCAGATATAAGAA
CXCR4	Forward	TCCAACAAGGAACCCTGCTTC
CXCR4	Reverse	TTGCCGACTATGCCAGTCAAG
CXCL1	Forward	CAATGAGCTGCGCTGTCAGT
CXCL1	Reverse	TTGAAGTGAATCCCTGCCACT

RT-qPCR was performed with the SYBR qPCR Kit and Applied Biosystems Step One Real-Time PCR system (Life Technologies, Gaithersburg, MD, USA). All primer pairs are listed in Table 1.

Enzyme-linked immunosorbent assay (ELISA)

TGF-β1, PDGF, VEGF, and CXCL12 ELISA kits (R&D systems, Minneapolis, MN, USA) were used to detect the concentrations of these cytokines in the serum according to the manufacturer's instructions.

Flow cytometry

Blood samples were collected in tubes containing EDTA-K2. Red blood cells were removed by the addition of RBC lysis buffer. The cells were washed and re-suspended, then incubated with the fluorescence-conjugated antibodies CD34 (clone HM34), CD133 (clone 315-2C11), and VEGFR2 (clone 89B3A5) (all purchased from BD Bioscience, Franklin Lakes, NJ, USA) for 20 min. The cells were analyzed with a BD flow cytometer (BD Biosciences, Franklin Lakes, NJ, USA).

Statistics analysis

The data are expressed as the mean ±SD. All data were analyzed using the unpaired t test between 2 groups and/or one-way analysis of variance (ANOVA) in multiple comparisons to determinate the significant differences, followed by post hoc test. A p value <0.05 was identified as significant. The results of statistics analysis are shown in Table 2. Graph Pad Prism v7.0 software (La Jolla, CA, USA) was used for data analysis.
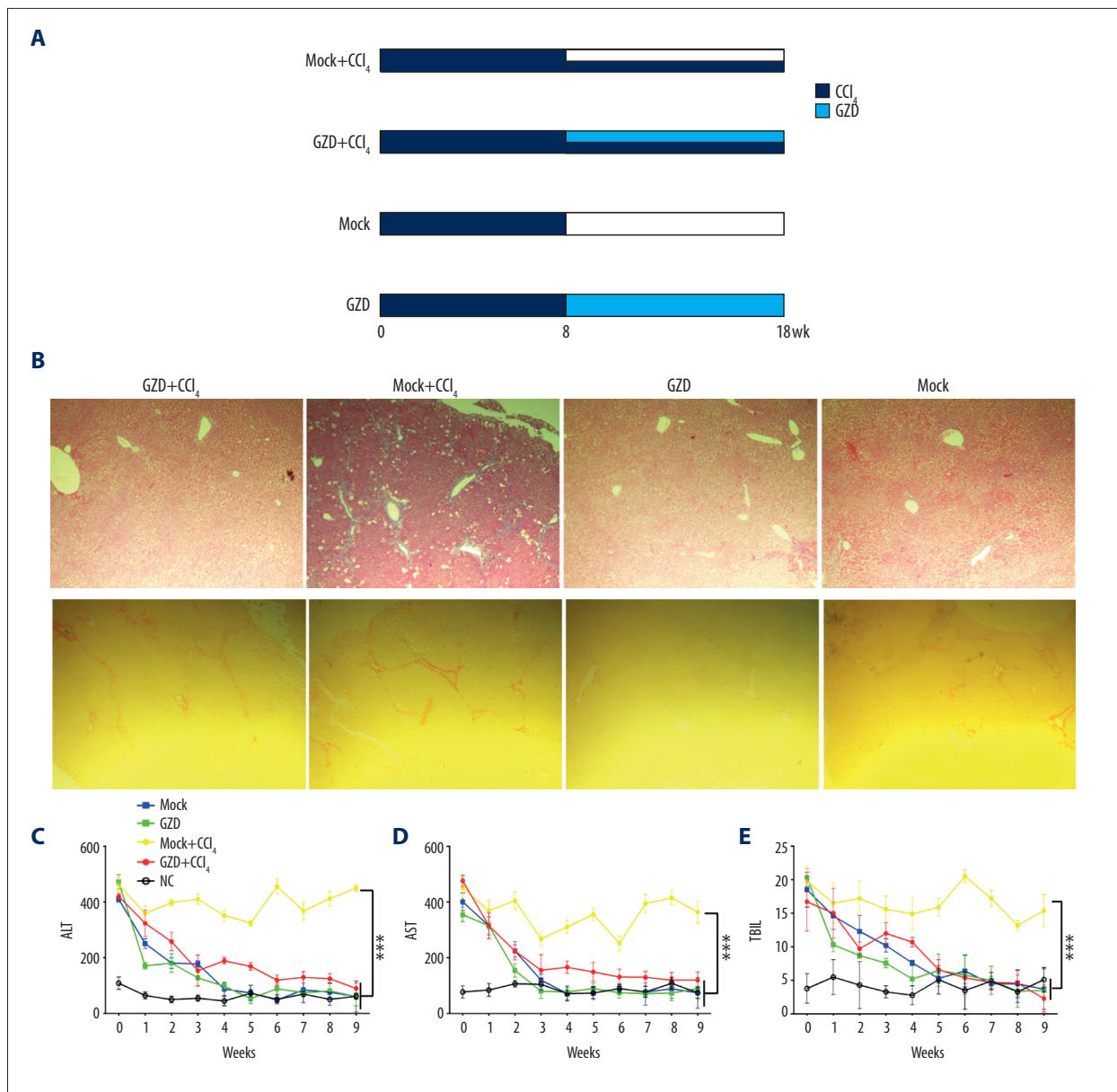
Table 2. The results of statistics analysis.

Figure number	NC *vs.* GZD+CCl4 (ANOVA test)	NC *vs.* Mock+CCl4 (ANOVA test)	GZD+CCl4 *vs.* Mock+CCl4 (Unpaired student's T test)
3B	p<0.001	p=0.0097	p=0.3041
3C	p<0.001	p<0.001	p=0.1076
3D	p=0.0024	p<0.001	p=0.0478
3E	p=0.5372	p=0.0078	p=0.0045
3F	p<0.001	p=0.1058	p=0.0336
4A	p=0.0045	p=0.0412	p=0.4752
4B	p=0.0160	p=0.7631	p=0.0047
4C	p=0.0041	p=0.4198	p=0.7521
5B	p=0.0047	p=0.4075	p=0.0047
5C	p<0.001	p<0.001	p=0.6041
5D	p<0.001	p=0.2058	p=0.0245

Figure 2. Administration of Gexia-Zhuyu decoction recovers liver function and prevents liver injury. (**A**) Timetable of animal experiment to detect the effect of GZD. (**B**) Representative histological images of Masson- and Sirius Red-stained liver sections. Kinetics of serum ALT (**C**), ASL (**D**), and TBIL (**E**). Data were pooled from 2 independent experiments (n=4–6). Graphs show mean and SD.

Results

Therapeutic administration of Gexia-Zhuyu decoction recovers liver function and attenuates collagen deposition in a CCl_4-induced liver fibrosis mouse model

To investigate the therapeutic efficacy of GZD treatment and identify the phase of recovery, the mice were treated as shown in Figure 2A. All mice were sacrificed at week 18, and the collagen deposition was measured by Sirius Red and Masson staining (Figure 2B). Discontinuation of the CCl_4 intervention at week 8 led to the recovery of liver fibrosis in GZD and Mock groups, suggesting that CCl_4-induced liver injury was reversible. In contrast, the mice that received continuous CCl_4 intervention in the Mock+CCl_4 group showed a severe collagen deposition and pathological alteration, demonstrating that GZD treatment significantly attenuates liver pathological alteration.

The serum AST, ALT, and TBIL concentrations, which indicate liver function, were measured weekly after the beginning of
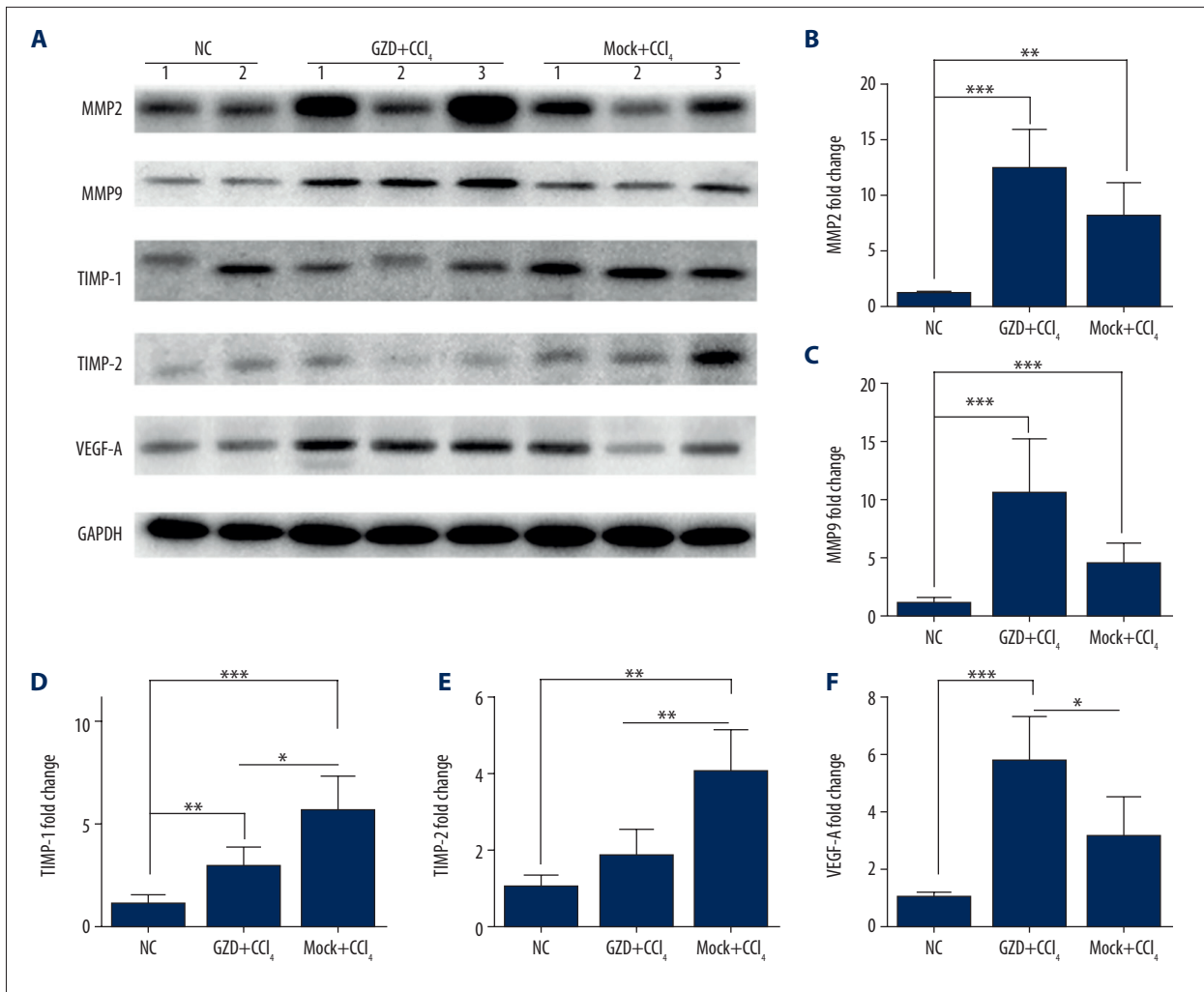
Figure 3. The increased MMPs and VEGF-A and decreased TIMPs were associated with the fibrosis resolution induced by GZD. (**A**) Protein levels of MMPs, VEGF-A, and TIMPs were detected by Western blot. The mRNA levels of MMP2 (**B**), MMP9 (**C**), TIMP1 (**D**), TIMP2 (**E**), and VEGF-A (**F**) in liver tissue were measured by RT-qPCR. Data were pooled from 2 independent experiments (n=4–6). Graphs show mean and SD. ANOVA test (*vs.* NC), ** $p<0.01$, *** $p<0.001$ or unpaired *t* test (GZD+CCl$_4$ *vs.* Mock+CCl$_4$), * $p<0.05$, ** $p<0.01$.

GZD treatment (Figure 2C–2E). The results indicated that the levels of serum AST, ALT, and TBIL in the GZD+CCl$_4$ group were significantly decreased as compared with that in the Mock+CCl$_4$ group, and returned to the normal level after 5 weeks of GZD administration. In addition, the mice without further CCl$_4$ intervention showed a spontaneous decrease of serum AST, ALT, and TBIL. In summary, these results demonstrate that GZD administration treated the CCl$_4$-induced fibrogenesis, and week 9 to 13 in this program was identified as the recovery phase.

Therapeutic administration of Gexia-Zhuyu decoction regulates extracellular matrix metalloproteinases/tissue inhibitors of metalloproteinase and increases hepatic VEGF-A level in the recovery phase

Deposition of ECM is a hallmark of liver fibrosis in chronic liver disease patients. To investigate the change in extracellular matrix metalloproteinases (MMP)/tissue inhibitors of metalloproteinase (TIMP) in the GZD treatment, we measured the hepatic TIMP1/2 and MMP2/9 levels in mice that received 3 weeks of GZD, which were experiencing recovery from liver fibrosis. Using Western blotting and RT-qPCR analysis, we found that the levels of MMP2/9 in the Mock+CCl$_4$ and GZD+CCl$_4$ groups were increased, but more significantly so in the GZD+CCl$_4$ group, suggesting that GZD induced a more potent degradation of ECM
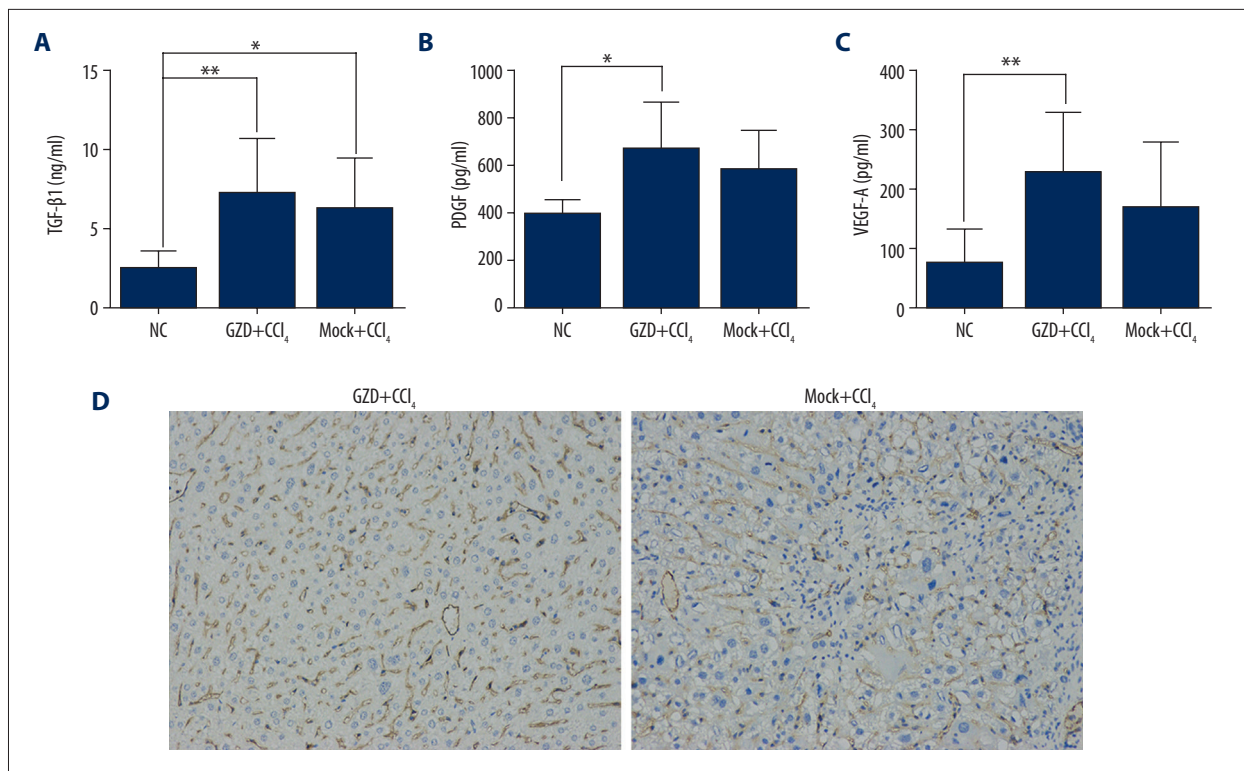
Figure 4. Systemic pro-angiogenic cytokines production induced by GZD administration contributed to the vascular regeneration. The protein levels of TGF-β1 (**A**), PDGF (**B**), and VEGF (**C**) in serum were measured by ELISA. (**D**) Paraffin-embedded sections were stained with CD31 (brown). Data were pooled from 2 independent experiments (n=4–6). Graphs show mean and SD. ANOVA test (*vs.* NC), * p<0.05, ** p<0.01.

in this time period. In contrast, although the levels of TIMP1 and TIMP2 were elevated in the GZD+CCl$_4$ group, the mice with CCl$_4$ intervention alone showed excessive expression of TIMP1 and TIMP2. Given that GZD treatment might active blood circulation to resolve fibrosis, and functional angiogenesis might have a role in this process, we also measured the expression of VEGF-A in the recovery phase. The level of VEGF-A in the GZD+CCl$_4$ group drastically increased and was significantly higher than in the Mock+CCl$_4$ group (Figure 3A–3F). These results suggest that enhancement of MMPs and inhibition of the TIMPs, as well as increased VEGF-A, are associated with GZD-induced resolution of liver fibrosis.

Systemic pro-angiogenic cytokines production induced by Gexia-Zhuyu decoction administration drove hepatic functional angiogenesis

Although increased levels of pro-angiogenic factors such as VEGF-A, platelet-derived growth factor (PDGF), and transforming growth factor-β1 (TGF-β1) have been found to be involved in the process of fibrogenesis, recent research suggests that the VEGF-A secreted by myeloid cells promotes the resolution of liver fibrosis in human and experimental animals. First, the levels of blood VEGF-A, PDGF, and TGF-β1 were measured by

ELISA in the mice that received 3 weeks of GZD. We found that these mice showed a significant increase of all 3 factors indicated above, but the Mock mice only showed an augmented TGF-β1 level in blood (Figure 4A–4C). Next, we performed the CD31 staining of liver tissue to investigate the morphology of liver vessels in the GZD+CCl$_4$ and Mock+CCl$_4$ groups. The liver vessels in the GZD+CCl$_4$ group showed few fibrotic scars and normal morphology, whereas the vessels and sinusoids in the scar tissue from the Mock+CCl4 group were aberrant and rarefied, and there was inflammatory cell infiltration (Figure 4D). In summary, our results indicate that GZD administration promotes the production of systemic pro-angiogenic factors to resolve liver fibrosis.

The activation of pro-angiogenic myeloid cells contributed to the resolution of liver fibrosis induced by Gexia-Zhuyu decoction administration

Given that endothelial progenitor cells (EPCs) play roles in the formation of functional blood vessels and in the re-establishment of sinusoidal endothelial cells, we assessed changes in blood EPCs (identified by surface markers CD34, CD133, and VEGFR2, Figure 5A) in the phase of fibrosis recovery. The recovery of liver fibrosis, induced by GZD treatment, was associated
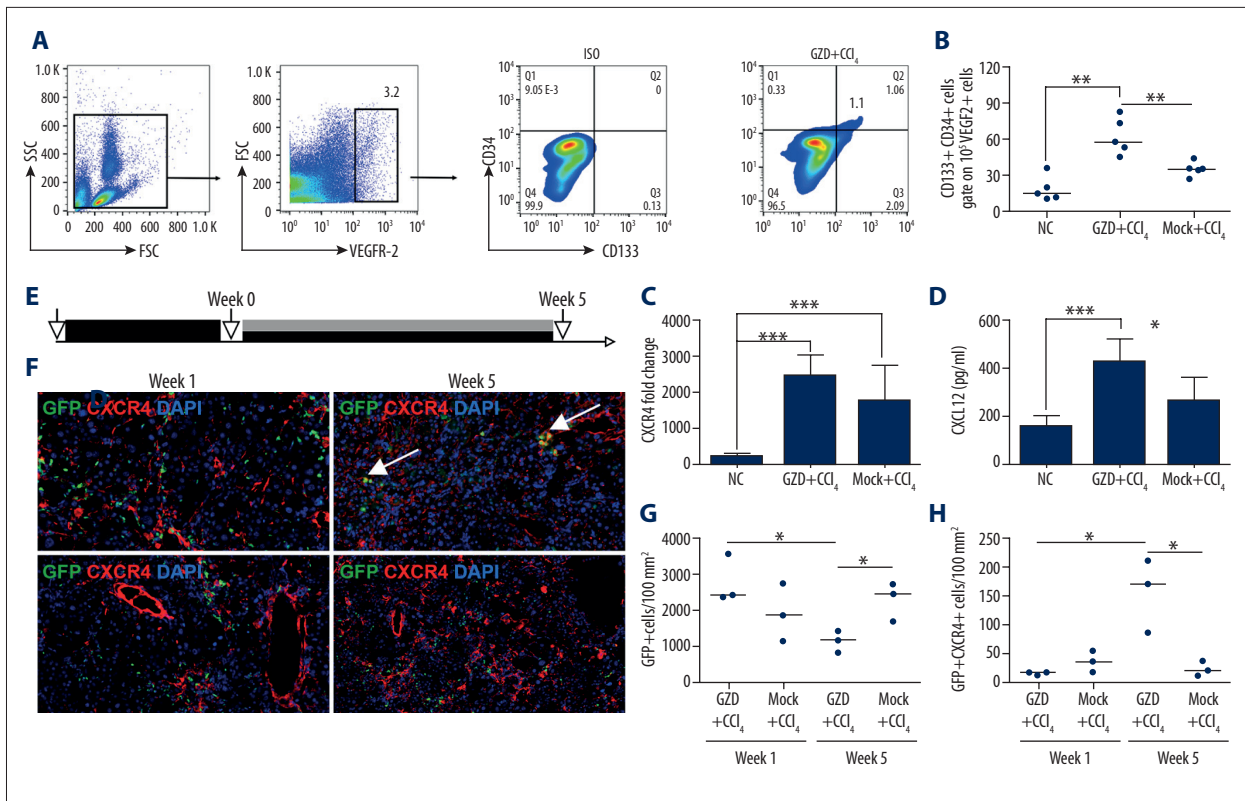
ANIMAL STUDY

Figure 5. Accumulation of pro-angiogenic myeloid cells in liver is associated with GZD-induced functional angiogenesis. (**A**) FACS analyses of CD34 and CD133 expression in VEGFR2+ cells in the peripheral blood. (**B**) The percentage of the CD34+CD133+ cells in VEGFR2+ cells were calculated. (**C**) The mRNA level of CXCR4 in liver tissue was measured by RT-qPCR. (**D**) The protein levels of CXCL12 were measured by ELSIA. Data were pooled from 2 independent experiments (n=5–6). Graphs shows mean and SD. ANOVA test (*vs.* NC), ** p<0.01, *** p<0.001 or unpaired *t* test (GZD+CCl$_4$ *vs.* Mock+CCl$_4$), * p<0.05, ** p<0.01. (**E**) Timetable of animal experiment to track the accumulation of pro-angiogenic myeloid cells in liver. (**F**) Frozen sections were stained with CXCR4 (red) and counterstained with DAPI (blue). The myeloid cells show as GFP-positive spots (green). Pro-angiogenic myeloid cells show as GFP and CXCR4 double-positive spots (yellow) in the GZD+CCl4 group (upper). The number of GFP+ (**G**) and GFP+CXCR4+ (**H**) cells in liver tissue were calculated in cross-section and normalized to an area of 100 mm^2. Data are presented as an independent experiment (n=3). Graphs showed mean. Unpaired *t* test, * p<0.05.

with augmented circulating EPCs (Figure 5B). Since the chemokine CXCL12/chemokine receptor CXCR4 pair in some cases contributes to activation of progenitor cells and drives vascular regeneration, we measured the expression of CXCR4 in liver and CXCL12 in blood (Figure 5C, 5D). In response to CCl$_4$ induced-liver injury, hepatic CXCR4 expression at the mRNA level was increased in mice treated with CCl$_4$. CXCL12, the cognate ligand of CXCR4, was significantly increased in the blood after treatment with GZD.

To further study the role of bone marrow cells in fibrosis recovery and the involvement of the CXCR4/CXCL12 axis, we constructed a bone marrow chimera mouse model by transplanting the bone marrow cells from eGFP mice into irradiated wild-type mice. The animal experiment was performed as shown in Figure 5E. The mice were sacrificed at week 1 and week 5 to track the bone marrow cells connected with functional angiogenesis (identified by eGFP and CXCR4 double-positive, Figure 5F).

We found low numbers of CXCR4+GFP+ cells at week 1 in both the Mock+CCl4 and GZD+CCl4 groups, but 5 weeks of GZD administration induced an augmented CXCR4+GFP+ subset in the liver, and these mice also showed fewer GFP+ cells, suggesting the resolution of inflammation (Figure 5G, 5H). Collectively, oral administration of GZD in mice triggered the mobilization of pro-angiogenic myeloid cells to resolve liver fibrosis.

Discussion

Traditional Chinese medicine has been used for thousands of years continues and is still widely used in East Asia. GZD is a traditional herbal medicine used for treating blood stasis and is also widely used in treating chronic active hepatitis, hematoporphyria, and diabetes. Studies on GZD treatment suggested that GZD administration shows potent effects in treating chronic HBV infection-induced liver fibrosis and preventing

platelet aggregation [10,11]. Previous research demonstrates that GZD treatment impedes the liver fibrosis induced by dimethylnitrosamine through inhibiting the proliferation of hepatic stellate cells, and, *in vitro*, GZT induces calcium release and apoptosis of LX-2 cells at a concentration of 300 µg/mL [8]. Additionally, paeoniflorin, the primary constituent of GZD, inhibits activated human monocytic cells producing intercellular adhesion molecule-1, which is parallel with the adhesive capacity of cells [12]. Another major constituent of GZD, glycyrrhizin, also shows multiple effects, such as anti-fibrosis, anti-inflammation, and hepatoprotective effects [13,14]. Empirically, based on the medical knowledge of traditional Chinese medicine, we hypothesized that GZD treatment acts on blood circulation to improve liver microcirculation and then relieve the symptom of liver fibrosis. We were particularly interested in whether functional angiogenesis plays a role in this process.

Pathological angiogenesis has been extensively described in chronic liver diseases and is considered to be one of the main causes of progression of fibrosis, mostly due to angiogenesis coexisting with pathological injury [15]. Progressive formulation of pathological vascular structure is associated with signaling molecules, which control the development of fibrosis and tissue hypoxia induced by distortion of organization structure [5,16]. Two signaling pathways are highlighted in the process of abnormal angiogenesis in liver fibrogenesis: first, over-expression of growth factors and MMPs with pro-angiogenic activity, including PDGF, TGF-β1, VEGF, integrins, and b-catenin; second, tissue hypoxia-induced blood vessel. However, recent evidence suggests that in the context of recovery, the functional angiogenesis may contribute to the resolution of liver fibrosis [7,17]. Indeed, activation of VEGFR2 in sinusoidal endothelium promotes liver repair and regulates the development of fibrosis [18]. A study on administration of VEGF neutralizing antibody demonstrated that VEGF induces fibrogenesis, and the resolution of fibrosis is dependent on the period of disease progression [17]. More recently, Kantari-Mimoun et al. [7] found that the mice lacking myeloid cell-derived VEGF display a defect in the spontaneous resolution of fibrosis, have decreased hepatic VEGF levels, and abrogate revascularization in the fibrotic region. Here, we traced the trail of previous studies and performed a dynamic study of liver function test with 10 weeks of GZD administration. The results suggest that 5 weeks of GZD administration is sufficient to reverse CCl4-induced liver injury. In this recovery phase, the level of pro-angiogenic factors in blood and VEGF-A in liver were increased in the mice that received GZD, and we found increased levels of MMP2 and MMP9 and reduced expression of TIMP1 and TIMP2. Thus, we speculated that GZD treatment might induce functional angiogenesis to resolve liver fibrosis.

A number of other studies support the role of bone marrow-derived cells in the functional angiogenesis that contributes to liver fibrosis resolution [19,20]. In fact, macrophages are important producers of VEGF and are involved in the formation of new blood vessels [21]. Additionally, a subset of myeloid cells, named EPCs, commits to endothelial cell formation, and EPCs transplant experiments show that EPCs can accumulate around the liver region of necrosis and ischemia, help the remodeling of sinusoidal endothelium, and then to some extent impede the process of fibrogenesis [22]. In the present study, administration of mice with GZD augmented the amount of blood EPCs, and enhanced blood CXCL12 content and hepatic CXCR4 expression. In a bone marrow chimera mouse model with GFP-positive myeloid cells, we found that continuous GZD administration promoted myeloid cell accumulation in liver and this was associated with sinusoidal CXCR4. The increased blood CXCL12 may attract myeloid cells (i.e., EPCs) to leave the bone marrow and home to the liver. The CXCL12/CXCR4 axis is critical for trafficking of progenitor cells from the bone marrow to the periphery [23,24]. Importantly, in response to the chronic injury caused by CCl$_4$ intervention, increased hepatic CXCR4 expression was observed in all experimental mice and provided a requirement for the blood progenitor cells homing to the liver. Additionally, CXCL12 level in blood and the GFP+CXCR4+ double-positive cells were significantly increased in the recipients of GZD+CCl$_4$, but not that of Mock+CCl$_4$, suggesting that administration of mice with GZD induced an effective action of myeloid cells into fibrosis resolution. This observation suggests that the engagement of GZD might drive a different pattern of functional angiogenesis that might break ECM deposition. Our future research will focus on whether GZD treatment can induce the resolution of human liver fibrosis in the same mechanism.

Conclusions

Our observations demonstrate that functional angiogenesis is driven by myeloid cells and VEGF-A contributes to the resolution of liver fibrosis induced by GZD treatment. This angiogenesis may repress the process of ECM deposition and be associated with the CXCL12/CXCR4 axis. This study shows the effect of GZD on the activation of myeloid cells and induces functional angiogenesis that accelerates fibrosis resolution.

Conflict of Interest

None.

References:

1. Iredale JP, Benyon RC, Pickering J et al: Mechanisms of spontaneous resolution of rat liver fibrosis. Hepatic stellate cell apoptosis and reduced hepatic expression of metalloproteinase inhibitors. J Clin Invest, 1998; 102: 538–49

2. Yang XZ, Gen AW, Xian JC, Xiao L: Diagnostic value of various noninvasive indexes in the diagnosis of chronic hepatic fibrosis. Eur Rev Med Pharmacol Sci, 2018; 22: 479–85

3. Jiao J, Friedman SL, Aloman C: Hepatic fibrosis. Curr Opin Gastroenterol, 2009; 25: 223–29

4. Fernandez M, Mejias M, Angermayr B et al: Inhibition of VEGF receptor-2 decreases the development of hyperdynamic splanchnic circulation and portal-systemic collateral vessels in portal hypertensive rats. J Hepatol, 2005; 43: 98–103

5. Hoofring A, Boitnott J, Torbenson M: Three-dimensional reconstruction of hepatic bridging fibrosis in chronic hepatitis C viral infection. J Hepatol, 2003; 39: 738–41

6. Onori P, Morini S, Franchitto A et al: Hepatic microvascular features in experimental cirrhosis: A structural and morphometrical study in CCl4-treated rats. J Hepatol, 2000; 33: 555–63

7. Kantari-Mimoun C, Castells M, Klose R et al: Resolution of liver fibrosis requires myeloid cell-driven sinusoidal angiogenesis. Hepatology, 2015; 61: 2042–55

8. Chen JY, Chen HL, Cheng JC et al: A Chinese herbal medicine, Gexia-Zhuyu Tang (GZT), prevents dimethylnitrosamine-induced liver fibrosis through inhibition of hepatic stellate cells proliferation. J Ethnopharmacol, 2012; 142: 811–18

9. Taniguchi E, Kin M, Torimura T et al: Endothelial progenitor cell transplantation improves the survival following liver injury in mice. Gastroenterology, 2006; 130: 521–31

10. She SF, Huang XZ, Tong GD: [Clinical study on treatment of liver fibrosis by different dosages of Salvia injection]. Zhongguo Zhong Xi Yi Jie He Za Zhi, 2004; 24: 17–20 [in Chinese]

11. Shi WR, Liu Y, Xie JD et al: [Changes in Wnt pathway inhibiting factors in nitrosamine-induced esophageal precancerosis lesions and effect of gexia zhuyu decoction]. Zhongguo Zhong Xi Yi Jie He Za Zhi, 2014; 39; 3131–35 [in Chinees]

12. Jin L, Zhang LM, Xie KQ et al: Paeoniflorin suppresses the expression of intercellular adhesion molecule-1 (ICAM-1) in endotoxin-treated human monocytic cells. Br J Pharmacol, 2011; 164: 694–703

13. Yan T, Wang H, Cao L et al: Glycyrrhizin alleviates nonalcoholic steatohepatitis via modulating bile acids and meta-inflammation. Drug Metab Dispos, 2018; 46(9): 1310–19

14. Abdel-Kader MS, Abulhamd AT, Hamad AM et al: Evaluation of the hepatoprotective effect of combination between hinokiflavone and Glycyrrhizin against CCl4 induced toxicity in rats. Saudi Pharm J, 2018; 26: 496–503

15. Thabut D, Shah V: Intrahepatic angiogenesis and sinusoidal remodeling in chronic liver disease: New targets for the treatment of portal hypertension? J Hepatol, 2010; 53: 976–80

16. Shackel NA, McGuinness PH, Abbott CA et al: Insights into the pathobiology of hepatitis C virus-associated cirrhosis: Analysis of intrahepatic differential gene expression. Am J Pathol, 2002; 160: 641–54

17. Yang L, Kwon J, Popov Y et al: Vascular endothelial growth factor promotes fibrosis resolution and repair in mice. Gastroenterology, 2014; 146: 1339–50

18. Ding BS, Cao Z, Lis R et al: Divergent angiocrine signals from vascular niche balance liver regeneration and fibrosis. Nature, 2014; 505: 97–102

19. Duffield JS, Forbes SJ, Constandinou CM et al: Selective depletion of macrophages reveals distinct, opposing roles during liver injury and repair. J Clin Invest, 2005; 115: 56–65

20. Leung DW, Cachianes G, Kuang WJ et al: Vascular endothelial growth factor is a secreted angiogenic mitogen. Science, 1989; 246: 1306–9

21. Stockmann C, Kerdiles Y, Nomaksteinsky M et al: Loss of myeloid cell-derived vascular endothelial growth factor accelerates fibrosis. Proc Natl Acad Sci USA, 2010; 107: 4329–34

22. Nakamura T, Torimura T, Sakamoto M et al: Significance and therapeutic potential of endothelial progenitor cell transplantation in a cirrhotic liver rat model. Gastroenterology, 2007; 133: 91–107

23. Doring Y, Noels H, van der Vorst E et al: Vascular CXCR4 limits atherosclerosis by maintaining arterial integrity: Evidence from mouse and human studies. Circulation, 2017; 136: 388–403

24. Doring Y, Pawig L, Weber C, Noels H: The CXCL12/CXCR4 chemokine ligand/receptor axis in cardiovascular disease. Front Physiol, 2014; 5: 212